Sources of error for single-shot PMT-based phosphor thermometry in harsh conditions

OPEN ACCESS
IOP Publishing
Measurement Science and Technology
Meas. Sci. Technol. **32** (2021) 084003 (7pp)
https://doi.org/10.1088/1361-6501/abfb1e

Sources of error for single-shot PMT-based phosphor thermometry in harsh conditions

Henrik Feuk*, David Sanned, Mattias Richter and Marcus Aldén

Combustion Physics, Lund University, Lund, Sweden

E-mail: henrik.feuk@forbrf.lth.se

Received 8 December 2020, revised 13 April 2021
Accepted for publication 23 April 2021
Published 13 May 2021

Abstract

This study investigates photomultiplier tube (PMT) nonlinearities, relevant for lifetime phosphor thermometry, at various decay times to assess and minimize the impact on temperature measurement accuracy. The focus is single-shot measurements performed in harsh environments where phosphor signal attenuation often is a concern. The sensitivity of decay time measurements to changing phosphorescence intensity is therefore investigated. The experimental results show that for the studied phosphors and detectors, shorter decay times between 20 ns and 6 μs, saturation effects in the PMTs decreased the measured decay time with increasing signal attenuation. For longer phosphorescence decay times, in the millisecond regime, nonlinearity effects led to an increase in the measured decay time with increasing signal attenuation. The specific detector nonlinearity response will vary among detectors, but the introduced methodology for detector analysis is a useful resource for assessing and improving accuracy in lifetime phosphor thermometry measurements.

Keywords: phosphor thermometry, photomultiplier tube, decay time, lifetime, surface temperature, lanthanides

(Some figures may appear in color only in the online journal)

1. Introduction

Temperature is one of the most fundamental and important variables when it comes to performance and reliability in almost any thermal system. This necessitates accurate, precise, and dependable temperature measurement methods.

Phosphor thermometry applies thermographic phosphors where the phosphorescence after excitation possesses a temperature dependence. This makes for a powerful remote, accurate and relatively non-intrusive measurement technique [1, 2].

The two most common approaches to phosphor thermometry are the intensity ratio and lifetime methods. In the intensity method, one uses the changes in intensity of two spectral regions to determine temperature. In the lifetime method, the temperature dependent phosphorescence decay time for a specific emission line is measured to extract temperature. Both these methods require calibration to give accurate temperature measurements.

The lifetime method is used in this study as it in general possesses better temperature precision at higher temperatures [3, 4]. A photomultiplier tube (PMT) based acquisition system is used as PMTs are highly sensitive and have fast rise and fall times which result in them being the most commonly applied point detector for lifetime phosphor thermometry [5].

There exist two main PMT effects that can introduce nonlinear detector response, namely photocathode bleaching and space charge accumulation at the end of the dynode chain. Photocathode bleaching arises when an excess of photons

* Author to whom any correspondence should be addressed.

reaches the photocathode within a sufficiently short time interval and depletes the valence band resulting in a nonlinear intensity response in the PMT. Space charge accumulation is more likely with high light fluence, high overall gain, and lower voltage configuration across the last dynodes in the PMT [6]. Such conditions can generate significant local electric fields (space charges) at the end of the dynode chain and the anode which disturbs incoming electrons. This limits the ability to convert incoming photons into an outgoing current and introduces another source of nonlinear response [6, 7].

Previous work has shown that the nonlinear PMT effects described can lead to considerable error in the measured decay time when the phosphorescence intensity changes. However, these earlier studies only investigated detection system effects at a fixed or slightly varying decay times. Furthermore, these studies did not always sufficiently decouple the effects due to changing phosphorescence intensity, PMT gain and laser fluence [6, 8–11]. The importance of decoupling these factors becomes evident when studying the relation between laser fluence and measured decay time. Detector nonlinearity effects due to changing phosphorescence intensity is best studied by attenuating the phosphorescence signal in a controlled manner. If one changes the phosphorescence intensity by changing the laser fluence of the excitation laser, then it is unclear whether detector effects or changes in the phosphorescence is the cause of changes in measured decay time.

This study investigates the effects of phosphorescence signal attenuation on the lifetime phosphor thermometry method. This is to provide guidance on how to minimize the impact of PMT nonlinearities on single-shot temperature measurements conducted in harsh environments. Harsh environment in the context of phosphor thermometry is here defined as an optically dense measurement environment where window fouling of optical access windows also may occur. These are conditions where laser pulse attenuation and phosphorescence attenuation are a concern. Measurements in combustion systems such as turbines and internal combustion engines often fall under the harsh environment category.

In this work, phosphor decay times ranging from 3 ms down to 20 ns are used to investigate their impact on nonlinearity effects in PMTs. This is investigated at four different gain settings for the PMTs to study what influence gain has on nonlinearity effects. The laser fluence was constant for all measurements in order to isolate detector effects from phosphor effects in the study.

The specific performance between different models of PMTs and even between individual PMTs of the same model will vary so the results presented may differ among detectors [10]. The purpose of this work is to emphasize the measurement situations where detector nonlinearities may lead to temperature errors and why they occur. The authors also present a methodology for assessing and improving temperature accuracy for lifetime phosphor thermometry measurements conducted in harsh environments.

2. Experimental setup

The experiments were performed with the phosphors YVO_4:Tm and Mg_3FGeO_6:Mn coated on different Hastelloy-C alloy disc-substrates, each connected to four type-K thermocouples for accurate temperature calibration; specifications are further described in [12]. Each of the phosphor powders (5% of weight) were mixed with ethanol (25% of weight) and a HPC binder from ZYP Coatings (70% of weight) and applied with an airbrush to produce a thin and homogeneous phosphor coating.

Figure 1 shows a schematic view of the experimental setup with the substrates placed in an optically accessible horizontal ceramic tube furnace. Both phosphors were excited by the third harmonic of a pulsed Nd:YAG laser at 10 Hz and a full width half maximum pulse duration of 5 ns.

The neutral density filters placed between the focusing lens and the PMT enabled the phosphorescence signal to be attenuated with great precision. The two PMTs used in this study were a non-gateable Hamamatsu H10721-01 and a gateable Hamamatsu H11526-20-NF, whose gate was always open during phosphor luminescence. The Hamamatsu H11526-20-NF PMT has a recommended control voltage range of 0.4–0.9 V and in this work the control voltage was varied between 0.2 and 0.8 V to include settings below the recommended limit that in previous work has been shown to be of interest [10]. Similarly, the control voltage of the Hamamatsu H10721-01 varied between 0.30 and 1.05 V with the recommended range of 0.5–1.1 V. Two different PMTs were utilized to reduce device specific performance effects with the aim to make the outcomes more general, however the most crucial aspect of the work is the methodology introduced. Both PMTs use a metal channel dynode type which gives short fall and rise times.

A 483 $\pm$ 31 nm bandpass filter (OD6 blocking between 250–455 nm and 510–660 nm) was used with the YVO_4:Tm phosphor to capture the $^1G_4$–$^3H_6$ transition around 475 nm [13]. For the Mg_3FGeO_6:Mn phosphor, this filter was replaced with a 656.3 $\pm$ 10 nm bandpass filter (average OD5 blocking for less than 581 nm and greater than 731 nm) to capture the ^2E–$^4A_2$ energy transition of the Mn^{4+} ion with a peak at 660 nm [14].

Mg_3FGeO_6:Mn was selected due to its frequent use within the field of phosphor thermometry and because its long decay time at ambient temperatures as seen in figure 2. YVO_4:Tm was selected due to its much stronger phosphorescence signal than Mg_3FGeO_6:Mn at decay times below 10^{-5} s. Together, their decay times span a range corresponding to multiple orders of magnitude while maintaining sufficient phosphorescence signal intensities for this study.

The decay profile of both phosphors is multi-exponential, and the degree of multi-exponentiality varies with temperature. A mono-exponential decay curve seen in equation (1) was fitted to the decay curves to remove the ambiguity of a multi-exponential method

$$I(t) = I_0 \cdot \exp(-t/\tau) + I_{\text{offset}}. \quad (1)$$

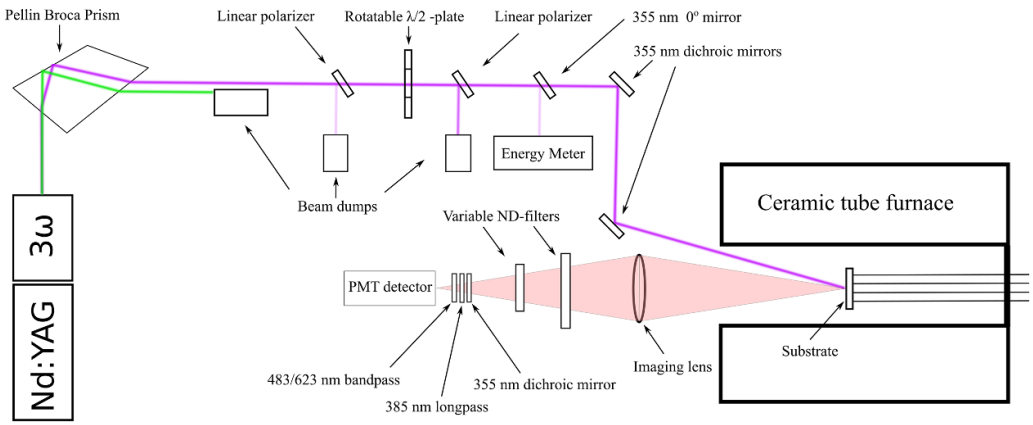

Figure 1. Experimental setup.

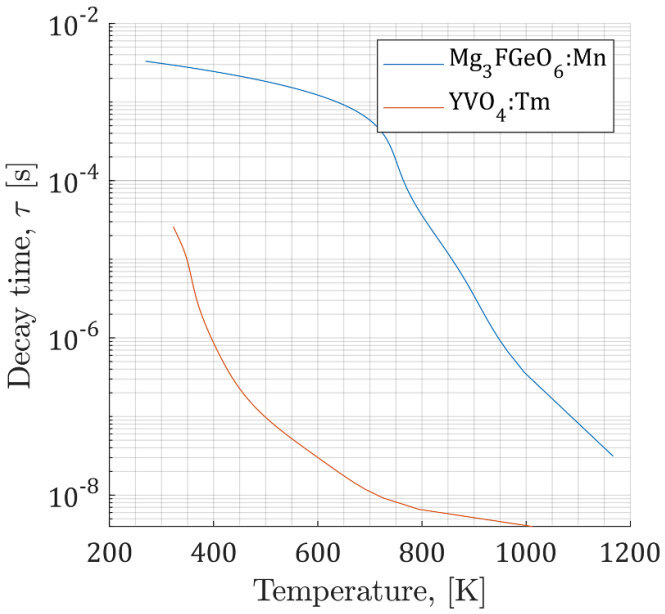

Figure 2. Calibration curves for the two phosphors using Hamamatsu H11526-20-NF PMT.

The mono-exponential decay curve was fitted using a trust-region-reflective least-squares algorithm in MATLAB. The start of the fitting window was at 71% percent of peak voltage and the end of the fitting window was 4% of the peak voltage. The calibration of the two phosphors was performed in a similar manner as in [12], with an average laser pulse energy of 1 mJ (1.6 mJ cm^{-2}). All measurements in the study used the same laser fluence.

Mg_3FGeO_6:Mn was evaluated at temperatures of 294, and 767 K corresponding to decay times 3×10^{-3}, and 10^{-4} s. Similarly, YVO_4:Tm was evaluated at temperatures of 345, 418 and 663 K corresponding to decay times of 6×10^{-6}, 3×10^{-7} and 2×10^{-8} s.

For every combination of detector, temperature, control voltage and phosphorescence signal level, 200 waveforms of the decay time were acquired, each sampled with a maximum of 10^4 data points.

3. Results and discussion

In figures 3 and 4, the fractional decay time error was calculated by dividing all the decay times within a decay time series (for example 3×10^{-3} s) by the decay time of the data point with the lowest peak signal in the same decay time series. The peak signal level for a decay curve is defined as the maximum voltage measured during the signal. The data point with the lowest peak signal was chosen as the reference point as it is assumed that the point with the lowest phosphorescence intensity will also experience the least detector nonlinearities. In figure 3 the measured decay time using the H11526-20-NF PMT is observed to decrease with increasing peak signal for decay times around 3×10^{-3} s. The maximum peak signal level with low gains is limited for the 3×10^{-3} s decay time series in particular because of the relatively low phosphorescence intensity of Mg_3FGeO_6:Mn at ambient temperatures. For decay times of 10^{-4} s no saturation effects can be seen. However, at decay times around 6×10^{-6} s, clear signs of saturation effects are visible, leading to the expected increase in measured decay time with peak signal level. Decay times shorter than 6×10^{-6} s showed reduced nonlinearity effects. Decay times at higher control voltages displayed increased noise due to only small fractions of the phosphorescence intensity being allowed to reach the detector to avoid excessive anode currents which could potentially damage the PMT.

For single-shot temperature measurements, the superior precision at lower gains due to a higher photon flux from a corresponding peak signal level is very attractive for the gateable PMT, but one needs to be mindful of potentially worse decay time accuracy.

Results from the conventional, non-gateable, H10721-01 PMT seen in figure 4, show significant nonlinearities in measured decay time with increasing peak signal level for decay times of 3×10^{-3} s. The detector suffers less from nonlinearities than the gateable detector at decay times of 6×10^{-6} s.

Figures 3 and 4 allows one to assess appropriate detector settings and peak signal levels for a given measurement situation. For both the detectors, the minimum recommended control voltage of 0.4 V for the gateable detector and 0.5 V for

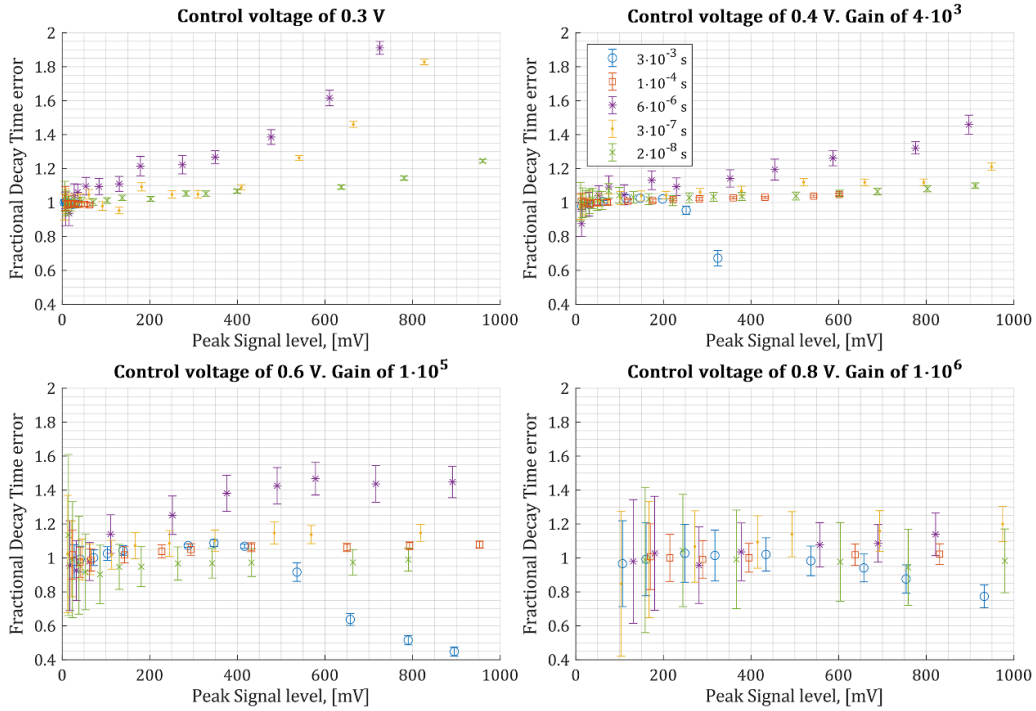

Figure 3. Decay time error versus peak signals using the gateable H11526-20-NF PMT with constant laser fluence for a range of decay times and control voltages. The peak signal was varied using neutral density filters.

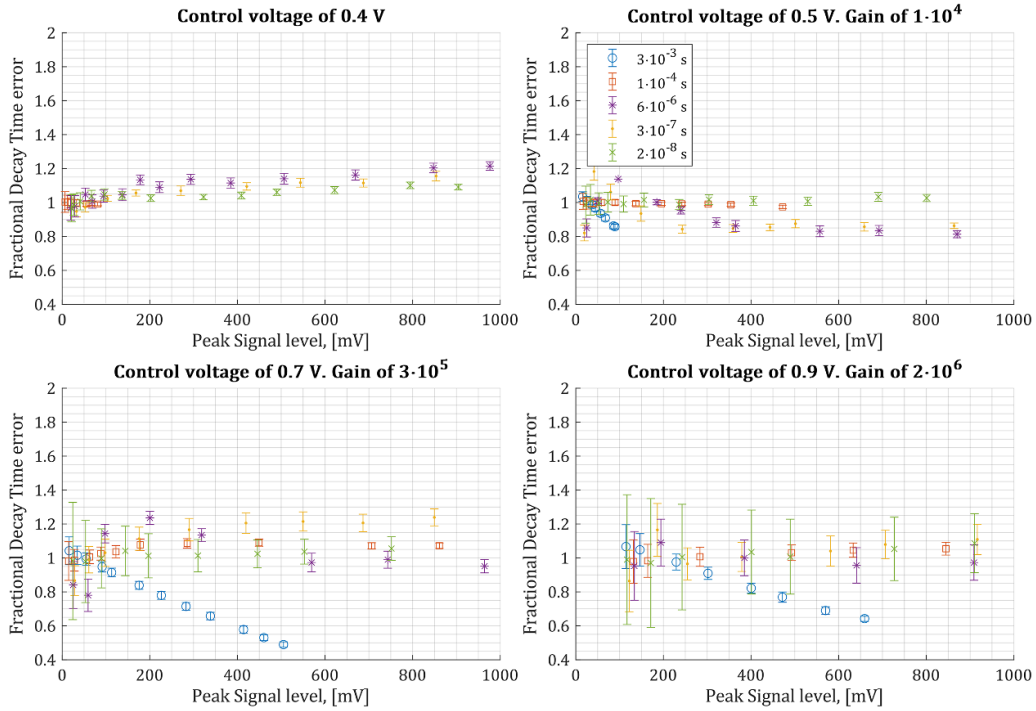

Figure 4. Decay time error versus different peak signals using non-gateable H10721-01 PMT with constant laser fluence for a range of decay times and control voltages. The peak signal was varied using neutral density filters.

the non-gateable detector results in a relatively good trade-off between linearity and decay time precision for single-shot measurements.

Two decay curve examples, using the H11526-20-NF PMT, were created to illustrate the correlation between peak signal level and the shape of the decay curve, shown in figures 5 and 6. In figure 5 a longer decay time can be observed for the 470 mV signal than for the 100 mV. The higher signal level in the 470 mV case probably leads to more significant space charge accumulation at the anode and the last few dynodes.

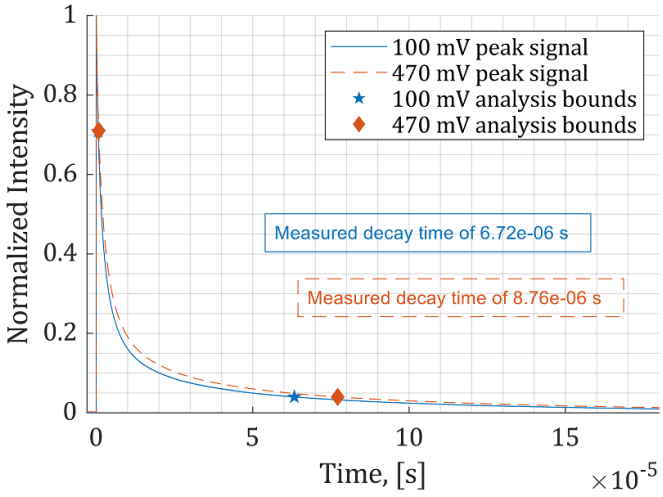

Figure 5. Change in decay curve due to different peak signals for approximately 6×10^{-6} s decay time at a control voltage of 0.3 V. Both decay curves are averages of 200 decay profiles.

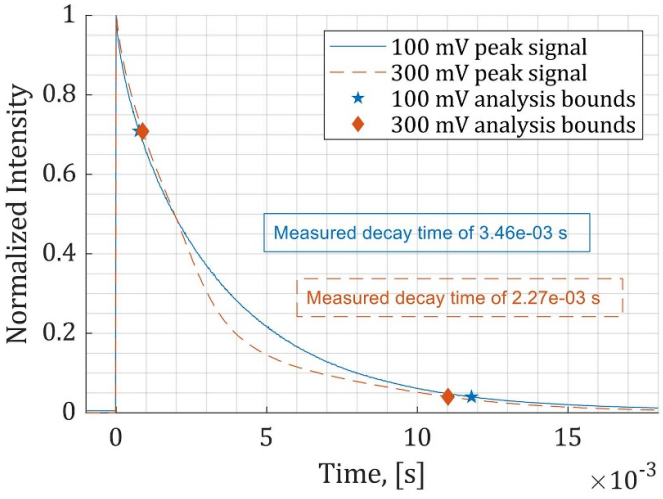

Figure 6. Change in decay curve due to different peak signals for approximately 3×10^{-3} s decay time at a control voltage of 0.4 V. Both decay curves are averages of 200 decay profiles.

Space charge accumulation disturbs the propagation of electrons and ultimately reduces the anode current and prolongs the signal leading to a longer perceived decay time [7]. The lower signal at 100 mV probably has a faster decay time due to reduced accumulation of space charges. The rapid decrease in signal intensity for the 300 mV signal after about 2 ms in figure 6 is probably due to photocathode bleaching. After bleaching, it takes some time for the photocathode to recover and return to a linear response again [7]. However, it may also be charge depletion in the PMT's dynode chain [15].

It appears that the photocathode or dynode chain recovers towards the end of the decay curve as the 300 mV signal moves closer to the 100 mV signal over time. The 300 mV decay curve is probably higher than the 100 mV signal until 2 ms due to space charge effects similar to what is seen in figure 5. After 2 ms, the photocathode bleaching, or dynode chain depletion becomes the dominant source of nonlinearity and the signal intensity rapidly falls.

The photocathode bleaching or dynode chain depletion resulted in a decrease in decay time with increasing peak signal for decay times in the millisecond regime and not for shorter decay times as seen in figures 3 and 4. This suggests that it takes a few milliseconds to manifest for the detectors and light fluences used. It is important to mention that there was negligible background illumination in this experiment and measurements performed with relevant background illumination may make photocathode bleaching and space charge effects even more important to consider.

The potential effect of detector nonlinearity on temperature determination can be seen in figures 7 and 8 with data acquired using the H11526-20-NF PMT. The temperature errors for the control voltage data series in figures 7(b) and 8(b) were calculated based on separate reference temperatures for each control voltage data series and figure. The reference temperature was the data point with the lowest average peak signal value for each control voltage data series and figure. The data point with the lowest peak signal is used as the reference point as it is assumed that the point with the lowest phosphorescence intensity also experiences the least detector nonlinearities. The temperature error therefore represents the change in measured temperature with increasing peak signal level. The data points for decay time and temperature error in figures 7 and 8 is the average value of 200 data points where the error bars represent the standard deviation in the data.

The small decay time error in combination with high sensitivity for Mg_3FGeO_6:Mn at 767 K results in minor temperature errors in figure 7. An increase in decay time with increasing peak signal is observed for control voltages between 0.4 and 0.8 V. No trend can be seen for a control voltage of 0.3 V due to low phosphorescence intensity.

For YVO_4:Tm at 663 K in figure 8 the decay time increases with increasing peak signal level for all studied control voltages, although less for the higher control voltages.

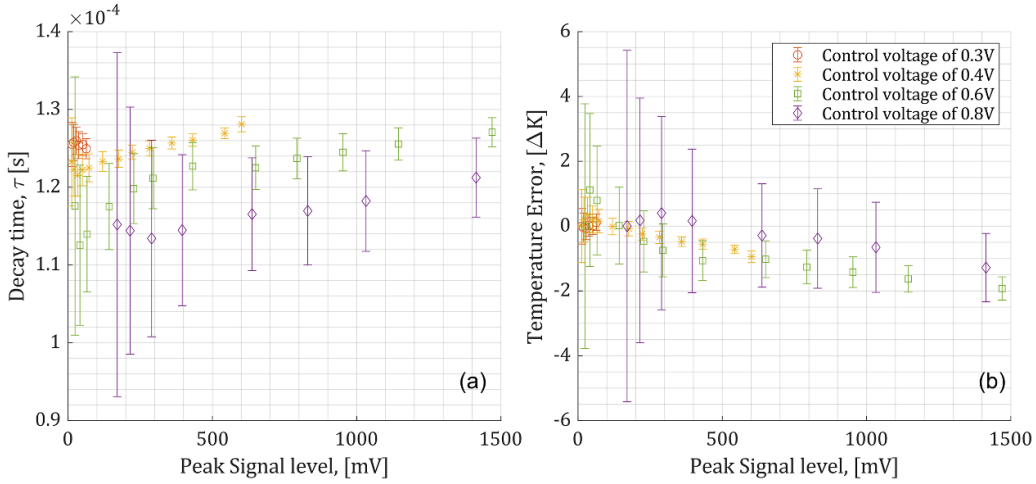

Figure 7. Decay time (a) and temperature measurement impact (b) for H11526-20-NF PMT with Mg_3FGeO_6:Mn at 767 K.

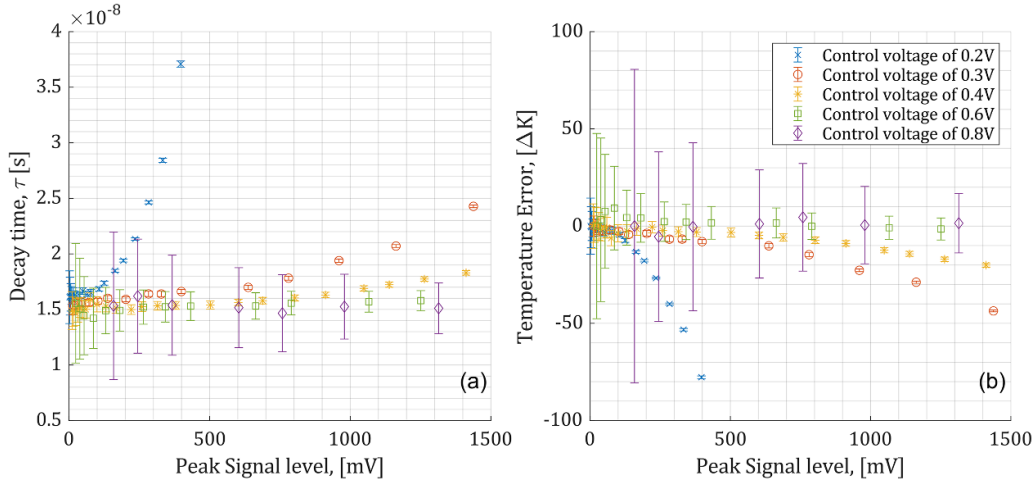

Figure 8. Decay time (a) and temperature measurement impact (b) for H11526-20-NF PMT with YVO_4:Tm at 663 K.

For control voltage of 0.2 V, far below the recommended minimum of 0.4 V, especially strong nonlinearity can be observed. This is likely due to collection efficiency dependence on light fluence when operating so far below the recommended control voltage [16].

4. Conclusions

This study showed that saturation effects with decay times in the milliseconds caused the measured decay time to be decreased with increased peak signal level. This could be explained by the PMTs' photocathode or dynode chain being bleached more at higher peak signal levels and as a result decreasing the signal for the later portion of the decay curve.

With shorter decay times, in the tens of nanoseconds to tens of microseconds, saturation effects in general increased the observed decay time with increased peak signal level, which likely is due to increased space charges accumulating within the PMTs.

These nonlinearities result in one needing to ensure that peak signal intensities are kept in the regime where decay time is predominantly insensitive to changing phosphorescence intensity for a given gain.

In general, the PMT study showed improved linearity with an increase in gain for a given peak signal level and decay time. Higher gains resulted in worse decay time precision, thus the choice of gain should be made based on a balance between precision and accuracy for a given application.

Another way to combat temperature errors is to use higher sensitivity phosphors which result in reduced temperature error caused by detector non-linearities.

The nonlinear response of any individual PMT will vary, but the methodology introduced allows for phosphor thermometry practitioners to assess and minimize temperature errors due to detector nonlinearities.

Data availability statement

The data that support the findings of this study are available upon reasonable request from the authors.

Acknowledgments

The authors would like to acknowledge funding from the Swedish Research Council/Swedish Energy Agency through Project 45400-01 and CECOST, funded by the Swedish Energy Agency.

ORCID iDs

Henrik Feuk https://orcid.org/0000-0003-2213-458X
David Sanned https://orcid.org/0000-0002-2213-3512

References

[1] Brübach J, Pflitsch C, Dreizler A and Atakan B 2013 On surface temperature measurements with thermographic phosphors: a review *Prog. Energy Combust. Sci.* **39** 37–60
[2] Aldén M, Omrane A, Richter M and Särner G 2011 Thermographic phosphors for thermometry: a survey of combustion applications *Prog. Energy Combust. Sci.* **37** 422–61
[3] Fuhrmann N, Brübach J and Dreizler A 2013 Phosphor thermometry: a comparison of the luminescence lifetime and the intensity ratio approach *Proc. Combust. Inst.* **34** 3611–8
[4] Brites C D, Balabhadra S and Carlos L D 2019 Lanthanide-based thermometers: at the cutting-edge of luminescence thermometry *Adv. Opt. Mater.* **7** 1801239
[5] Allison S W and Gillies G T 1997 Remote thermometry with thermographic phosphors: instrumentation and applications *Rev. Sci. Instrum.* **68** 2615–50
[6] Knappe C, Lindén J, Abou Nada F, Richter M and Aldén M 2012 Investigation and compensation of the nonlinear response in photomultiplier tubes for quantitative single-shot measurements *Rev. Sci. Instrum.* **83** 034901
[7] Hartman D H 1978 Pulse mode saturation properties of photomultiplier tubes *Rev. Sci. Instrum.* **49** 1130–3
[8] Lindén J, Knappe C, Richter M and Aldén M 2012 Limitations of ICCD detectors and optimized 2D phosphor thermometry *Meas. Sci. Technol.* **23** 035201
[9] Knappe C, Nada F A, Richter M and Aldén M 2012 Comparison of photo detectors and operating conditions for decay time determination in phosphor thermometry *Rev. Sci. Instrum.* **83** 094901
[10] Nada F A, Knappe C, Aldén M and Richter M 2016 Improved measurement precision in decay time-based phosphor thermometry *Appl. Phys.* B **122** 170
[11] Persvik Ø, Melø T B and Naqvi K R 2013 Pulsed-source time-resolved phosphorimetry: comparison of a commercial gated photomultiplier with a specially wired ungated photomultiplier *Photochem. Photobiol. Sci.* **12** 1110–3
[12] Nada F A, Knappe C, Xu X, Richter M and Aldén M 2014 Development of an automatic routine for calibration of thermographic phosphors *Meas. Sci. Technol.* **25** 025201
[13] Zhang H, Fu X, Niu S, Sun G and Xin Q 2004 Photoluminescence of YVO_4:Tm phosphor prepared by a polymerizable complex method *Solid State Commun.* **132** 527–31
[14] Brübach J, Feist J P and Dreizler A 2008 Characterization of manganese-activated magnesium fluorogermanate with regards to thermographic phosphor thermometry *Meas. Sci. Technol.* **19** 025602
[15] Vander Wal R L, Householder P A and Wright T W 1999 Phosphor thermometry in combustion applications *Appl. Spectrosc.* **53** 1251–8
[16] HAMAMATSU Photonics 2017 *Photomultiplier Tubes Basics and Application* 4th edn